POLITECNICO DI TORINO
Repository ISTITUZIONALE

Leveraging re-chargeable nanobubbles on amine-functionalized ZnO nanocrystals for sustained ultrasound cavitation towards echographic

Original
Leveraging re-chargeable nanobubbles on amine-functionalized ZnO nanocrystals for sustained ultrasound cavitation towards echographic / Ancona, A., Troia, A., Garino, N., Dumontel, B., Cauda, V.A., Canavese, G.. - In: ULTRASONICS SONOCHEMISTRY. - ISSN 1350-4177. - ELETTRONICO. - (2020), p. 105132. [10.1016/j.ultsonch.2020.105132]

Availability:
This version is available at: 11583/2815896 since: 2020-04-24T09:20:08Z

Publisher:
Elsevier

Published
DOI:10.1016/j.ultsonch.2020.105132

Terms of use:

This article is made available under terms and conditions as specified in the corresponding bibliographic description in the repository

Publisher copyright

(Article begins on next page)

25 November 2026

Journal Pre-proofs



Leveraging re-chargeable nanobubbles on amine-functionalized ZnO nanocrystals for sustained ultrasound cavitation towards echographic imaging

Andrea Ancona, Adriano Troia, Nadia Garino, Bianca Dumontel, Valentina Cauda, Giancarlo Canavese

PII: S1350-4177(19)31381-1
DOI: https://doi.org/10.1016/j.ultsonch.2020.105132
Reference: ULTSON 105132

To appear in: *Ultrasonics Sonochemistry*

Received Date: 3 September 2019
Revised Date: 27 February 2020
Accepted Date: 15 April 2020

Please cite this article as: A. Ancona, A. Troia, N. Garino, B. Dumontel, V. Cauda, G. Canavese, Leveraging re-chargeable nanobubbles on amine-functionalized ZnO nanocrystals for sustained ultrasound cavitation towards echographic imaging, *Ultrasonics Sonochemistry* (2020), doi: https://doi.org/10.1016/j.ultsonch.2020.105132

This is a PDF file of an article that has undergone enhancements after acceptance, such as the addition of a cover page and metadata, and formatting for readability, but it is not yet the definitive version of record. This version will undergo additional copyediting, typesetting and review before it is published in its final form, but we are providing this version to give early visibility of the article. Please note that, during the production process, errors may be discovered which could affect the content, and all legal disclaimers that apply to the journal pertain.

© 2020 Published by Elsevier B.V.

Journal Pre-proofs

Leveraging re-chargeable nanobubbles on amine-functionalized ZnO nanocrystals for sustained ultrasound cavitation towards echographic imaging

Andrea Ancona, Adriano Troia, Nadia Garino, Bianca Dumontel, Valentina Cauda and Giancarlo Canavese*

Ing. A. Ancona, Dr. N. Garino, Ing. B. Dumontel, Prof. V. Cauda and Ing. Dr. G. Canavese, Department of Applied Science and Technology, Politecnico di Torino
C.so Duca degli Abruzzi 24, 10129 Turin, Italy
E-mail of corresponding author: valentina.cauda@polito.it

Dr. A. Troia, Ultrasounds & Chemistry Lab, Advanced Metrology for Quality of Life, Istituto Nazionale di Ricerca Metrologica (I.N.Ri.M.) Strada delle Cacce 91, 10135 Turin, Italy

Keywords: Zinc Oxide, Nanoparticles, Ultrasound, Cavitation, Contrast agent, Nanobubbles

Abstract

Nanoparticles able to promote inertial cavitation when exposed to focused ultrasound have recently gained much attention due to their vast range of possible applications in the biomedical field, such as enhancing drug penetration in tumor or supporting ultrasound contrast imaging. Due to their nanometric size, these contrast agents could penetrate through the endothelial cells of the vasculature to target tissues, thus enabling higher imaging resolutions than commercial gas-filled microbubbles. Herein, Zinc Oxide NanoCrystals (ZnO NCs), opportunely functionalized with amino-propyl groups, are developed as novel nanoscale contrast agents that are able, for the first time, to induce a repeatedly and over-time sustained inertial cavitation as well as ultrasound contrast imaging. The mechanism behind this phenomenon is investigated, revealing that re-adsorption of air gas nanobubbles on the nanocrystal surface is the key factor for this re-chargeable cavitation. Moreover, inertial cavitation and significant echographic signals are obtained at physiologically relevant ultrasound conditions (MI<1.9), showing great potential for low side-effects in in-vivo applications of the novel nanoscale agent from diagnostic imaging to gas-generating theranostic nanoplatforms and to drug delivery.

Journal Pre-proofs

1. Introduction

To enable early disease detection and therapy monitoring, molecular imaging promises to expand the range of functional imaging, and ultrasound may be a useful tool [1]. To guarantee the required stability and high ultrasound scattering behaviour, the clinically-approved contrast agents have a size of several microns and their potential application of molecular imaging is limited to the vascular compartment, since the extravasation is prevented by their dimensions [2]. The key point to provide spatial information for imaging-guided biopsy and to extend the use of ultrasound molecular imaging to solid tumours will be the development of nano-contrast agents (i.e. smaller than 600 nm) [3-5] capable to extravasate and maintain a high stability [6-8]. However, this last constraint bumps against the thermodynamic instability of nanobubbles (i.e. fine bubbles) [9]. Actually, several numerical and analytical models predict the bulk nanobubbles in pure water as thermodynamically instable entities with lifetime in the range of few microseconds [10]. This is namely the Laplace pressure bubble catastrophe [11] which in principle discourages any attempt to apply the bulk nanobubbles technology to any fields requiring long term stability, such as the ultrasound contrast agent for medical applications [10]. By designing specific boundary conditions, various experimental approaches have attempted to demonstrate the lifetime extension of bulk nanobubbles [12, 13]. In this way, their high interface energy, together with their high surface area per volume and easy dissolution are leveraged. Bulk nanobubbles have been recently proved to exist and get stabilized over long period of times [14-16]. Furthermore, there are experimental evidences to stabilize bulk nanobubbles on surfaces, thus creating stable surface nanobubbles, shed light on the development of a new class of contrast agents able to leverage the stability of these nanosized entities to generate sustained echogenic signals. This effect was experimentally demonstrated with various nanoparticle seeds, including hydrophobic mesoporous silica nanoparticles [17] and solid polymeric nanoparticles (PTFE) [18-20] able to immobilize surface nanobubbles to act as cavitation nuclei under ultrasound stimulation.

Different works conducted on mesoporous silica nanoparticles established the importance of hydrophobicity and surface roughness or porosity to trap and stabilize gas against dissolution in the fluid, and indicated cavitation threshold dependence on the presence and size of crevices, surface chemistry, and amount of impurities [10, 21, 22]. Other experiments developed by employing different solvents (i.e. ethanol) or capping agent (i.e. bovine serum albumin, or cyclodextrin) proved that acoustic cavitation is principally nucleated by the nanobubbles stabilized at the nanoparticle surface and not into the mesopores [23]. Unfortunately, the nano-contrast agents proposed so far show various drawbacks, i.e. high acoustic pressures used [24], short duration of the US contrast signal or low biocompatibility, thus limiting their potential employment for in-vivo applications [25]. Herein, we present a novel ultrasound nano-contrast agent based on surface nanobubbles adsorbed on ZnO single-crystalline nanoparticles, i.e. ZnO NanoCrystals (ZnO NCs) [26, 27]. We have successfully designed the nano-contrast agent, including an amine-propyl surface functionalization, to overcome all the intrinsic limits observed so far in the literature. Indeed, these ZnO NCs can maintain long term stability in liquids (more than six months) with adsorbed gas pockets on their surface. Actually, the amino-propyl functionalization provides a positively-charged surface useful to improve the colloidal stability of the NCs in solution [28]. Inertial cavitation and significant echographic signal are achieved by ultrasound excitation at safe mechanical index (MI<1.9) [29] and maintained for extended time (>30min). Furthermore, for the first time we demonstrate a repetitive activation of the contrast agent

signal, that can thus be perpetually restored, paving the way to a single dose for intermittent and multi-section molecular imaging without the need of further administration.

2. Materials and Methods

2.1 Synthesis and functionalization of ZnO nanocrystals

ZnO NCs were synthesized through a microwave-assisted synthesis, as previously reported [28]. The reaction path is based on the hydrolysis of the zinc precursors due to the presence of the hydroxide. The as-synthesized ZnO NCs were then functionalized with amino-propyl groups, as already shown previously [28].

2.2 Characterization of ZnO NCs

The morphology of the nanocrystals was studied by FESEM (Merlin, Karl Zeiss, Oberkochen, Germany) by spotting the diluted samples on a silicon wafer. Transmission electron microscopy (TEM) was performed by using a FEI Titan ST microscope working at an acceleration voltage of 300 kV, equipped with a S-Twin objective lens, an ultra-bright field emission electron source (X-FEG) and a Gatan 2k x 2k CCD camera. All the ZnO NCs samples were diluted in ultrapure ethanol (99%) down to a concentration of 100 μg/ml. One drop of each sample was deposited on a holey carbon copper grid with 300-carbon mesh and left to dry overnight, prior to imaging.

The particle size and Zeta potential of the samples were determined using the DLS technique (Zetasizer Nano ZS90, Malvern), using a concentration of 100 μg/mL of nanocrystals and sonicating each sample for 10 minutes before the acquisition. The crystalline structure was analyzed by XRD with a X'Pert diffractometer in θ-2θ Bragg-Brentano configuration using a Cu-K_α radiation (λ=1.54 Å, 40 kV, 30 mA). Nitrogen sorption isotherms were performed with Quadrasorb SI instrument (Quantachrome). Multipoint BET surface area was measured within the relative pressure range of p/p_0 = 0.1- 0.3. Barrett–Joyner–Halenda (BJH) equilibrium model was also used to estimate the pore volume and the pore size distribution of the samples.

2.3 PCD detection of cavitation activity

Ultrasound excitation was provided by a single-element home-made focused ultrasound transducer placed in a water bath orthogonal to the sample and driven at the fundamental harmonic (f=985KHz). All reported acoustic pressures are PRP measured using a *pvdf*-needle hydrophone (SN2195, sensor diameter 1.0mm) from Precision Acoustic, coupled to an oscilloscope (Agilent DSO-X2022A) and stored on PC using Labview software. The 1 mL solution composed by the NCs and milli-Q water was placed inside a single plastic 24-well used for cell cultures. The characterization of the acoustic cavitation inception by nanocrystals was tested by recording the broad band acoustic emissions generated by collapsing bubbles using a focused PCD centered at 5MHz frequency (Precision Acoustics), five times the main ultrasound excitation. The foci of both transducers were adjusted to overlap at the same position. The IC signal was received and amplified by 25dB hydrophone booster amplifier (Precision Acoustics), and then recorded by a digital oscilloscope (TDS2012B). The recorded time-domain signal acquired at sampling rate of 1 Gsamples/s was first transformed into a frequency domain spectrum A(f) using Fast Fourier Transform. Then the integral values of area under the frequency spectrum 2-10MHz was calculated and termed as cavitation dose (V/Hz), which can be used to assess the IC intensity.

2.4 Ultrasound imaging

US imaging was performed with a research ultrasonic scanner (Ultrasonix Sonic Touch) equipped with linear probe (L14-5/38) operating at 10MHz in high resolution B-mode and coupled using commercial ultrasound gel. The imaging transducer was aligned to the excitation transducer focus. Real-time videos of the system response to ultrasound irradiation were recorded. Videos were analyzed using MATLAB which calculated the relative average intensity of the bright spots in the region of interest (ROI) of each frame of the videos. Three videos were recorded for each sample.

2. Results and Discussion

3.1 ZnO nanocrystals Synthesis, Functionalization and Characterization

ZnO NCs were synthesized by a microwave-assisted synthesis, as recently reported [28]. In Figure 1a the Field Emission Scanning Electron Microscopy (FESEM) image shows nanoparticles with a spherical shape and an average diameter of 20±5 nm (measured using Fiji software, n=20). X-ray diffraction (XRD) pattern (Figure 1d, black spectrum) confirms the crystalline structure of ZnO NCs, corresponding to a wurtzite lattice. The amino-propyl functionalized NCs (ZnO-NH_2 NCs) also show a spherical morphology and a crystalline structure (Figures 1b and 1d, red spectrum, respectively), with a slightly larger size (average diameter of 21±5 nm) than pristine ZnO NCs. Furthermore, the TEM image (Figure 1e) reports on the single crystalline nature of the amine-fucntionalized ZnO NCs. As it is possible to observe from the TEM image, no porosity on the NCs surface is present, whereas the ZnO nanocrystals possess a compact and pore-free structure, as well as a single-crystalline wurtzite habit. We additionally performed the nitrogen (N_2) adsorption/desorption isotherm analysis (see Figure S1 in the Supporting Information), in order to estimate the surface area and pore volume related to the ZnO NCs in the dry form. The adsorption isotherm indicates the presence of interparticle porosity, formed by the close packing of the single nanocrystals in the dry state. The major of pore-size distribution is positioned above 15 nm: compared with the small size of the ZnO NCs, as assessed above, we can confirm that the presence of pores is strictly related to the space between the various ZnO NCs in the dry sample, i.e. an interparticle porosity. Furthermore, the measured specific surface area was of 61 m^2/g, thus showing a broad and accessible surface area due to the small particle size of the ZnO NCs.

The amino-propyl groups induce an increase of Z-potential values up to +22mV, from +16mV recorded for pristine ZnO NCs in ultrapure water at pH7 (Figure 1c). The absence of micrometer-size aggregates in Dynamic Light Scattering (DLS) data (Figure 1f) suggests a good dispersion and low aggregation behaviour for both samples with a larger mean hydrodynamic diameter (107 nm) of the ZnO-NH_2 NCs than the one obtained for pristine ZnO NCs (58 nm), as previously reported [28, 30]. Since the hydrodynamic diameter represents not only the size of a nanoparticles or of a group of aggregated nanoparticles, but also the first layers of adsorbed ions and molecules on their surface when immersed in a fluid, we can assume that the ZnO NCs, both pristine and amine-functionalized ones, can slightly aggregate in water solution, in a group of 2-3 NCs leading to the interparticle pores, which can play an active role, together with other parameters discussed below, as nucleation sites for the nanobubbles.

3.2 Passive cavitation detection of acoustic activity of bare and amino-propyl functionalized ZnO NCs

Passive acoustic cavitation detection (PCD) technique was used to characterize the ability of pristine and ZnO-NH_2 NCs to induce inertial cavitation under focused ultrasound excitation. By recording the acoustic emissions generated by the ultrasound-exposed sample, PCD technique allows the detection

and characterization of cavitation. ZnO nanocrystals (at a concentration of 200 μg/mL) were exposed to a single 100-cycles burst of ultrasound at 985 KHz frequency at a Peak Rarefactional Pressure (PRP) of 1.8 MPa. In the presence of ZnO-NH_2 nanocrystals, a strong broad-band acoustic emission typical of inertial cavitation was recorded (Figure 2a). Lower broad-band acoustic emissions were recorded for both pristine ZnO NCs solution and water. Varying the applied PRP from 0.4 to 2 MPa, the ZnO-NH_2 NCs promoted detectable inertial cavitation dose for PRP as low as 0.8 MPa, while water and ZnO NCs solutions induced inertial cavitation dose only for pressures above 1.6 MPa (Figure 2b). Figure 2c shows the cavitation dose obtained by varying the ZnO-NH_2 NCs concentration from 12.5 μg/mL up to 400 μg/mL. As expected, the inertial cavitation activity increased at increasing NCs concentration, reaching a plateau at 200 μg/mL. This can be explained by the scattering of the acoustic radiation operated by the nanocrystals: actually, NCs closer to the radiation source decrease the actual acoustic pressure reaching farther nanocrystals, producing a destructive interference, and thus eventually reducing the actual number of nanocrystals able to promote inertial cavitation. Collectively, these measurements demonstrate that the amino-propyl functionalization increases the ability of ZnO NCs to induce inertial cavitation. Furthermore, the ZnO-NH_2 nanocrystals are able to support inertial cavitation at acoustic pressure as low as 0.8 MPa, where neither water nor pristine ZnO nanocrystals generated cavitation. The next set of experiments will be devoted to investigate the mechanism behind this phenomenon.

3.3 Role of gas nuclei on the cavitation activity

Previous works have shown that surfaces able to trap gas within a nanoscale crevice are capable of generating a cavitation bubble after exposure to ultrasound [31, 32]. To investigate the possibility that the induction of inertial cavitation by ZnO-NH_2 nanocrystals was due to nanobubbles adsorbed at their surface, two methods were applied to remove the potentially adsorbed gas. The first strategy involves the addition of 90 %v/v pure ethanol into the ZnO-NH_2 NCs dispersion (200 μg/mL). Low surface energy liquids, such as alcohols, are known to wet the hydrocarbon-coated hydrophobic particles and surfaces [12], thus destroying surface nanobubbles and exchanging with the entrapped gas [33]. In the second strategy, vacuum was applied for 10 minutes on the ZnO-NH_2 NCs solution and maintained during the experiment to avoid gas reentering the chamber. As reported in Figure 3, the obtained cavitation doses for both ethanol solution (grey bar) and degassed sample (green bar) are drastically reduced compared to the non-treated solution (red bar). These results demonstrate that the induction of inertial cavitation is originated from the bubble nuclei adsorbed at the ZnO-NH_2 nanocrystals surface.

To further elucidate the role of gas nanobubbles adsorbed at the surface of the nanocrystals on the induction of inertial cavitation, a specific ultrasound sequence was designed (inset in Figure 4a). This is composed of 6 subsequent 100-cycles-pulses applied to pure water as well as to the pristine and amino-propyl functionalized ZnO NCs solutions with a Pulse Repetition Frequency (PRF) of 1 Hz and PRP of 1.6 MPa. Acoustic cavitation was recorded during each pulse by PCD technique. Interestingly, as shown in Figure 4a and 4b, inertial cavitation rapidly decreased at succeeding pulses, completely disappearing after the third 100-cycles pulse. These results suggest that, during the first 100-cycles pulse of ultrasound exposure, the layer of adsorbed gas on the nanocrystal surface detached and collapsed giving rise to the detected inertial cavitation. Then, at the second pulse, the nanocrystal surface had much less gas adsorbed onto it, thus generating much less inertial cavitation. During subsequent pulses, since no gas remained adsorbed at the nanocrystal surface, no

inertial cavitation was detected. This result further confirms the hypothesis that the amino-propyl functionalization is able to increase the amount of adsorbed gas layer over the ZnO NCs surface, thus increasing their ability to induce inertial cavitation.

3.4 Insights into the cavitation-induction mechanism

To get further insights into the mechanism behind the induction of inertial cavitation by the adsorbed gas, we hypothesize that the gas pockets can be detached from the NC surface forming an unstable bulk nanobubble in solution. Once detached, if the nanobubble is exposed to a PRP higher than its cavitation threshold, it will collapse generating broad band noise typical of inertial cavitation. If instead it is exposed to lower PRPs, it will dissolve due to Laplace Pressure Catastrophe. To investigate this hypothesis, the ZnO-NH_2 NCs were first exposed to continuous ultrasound using a PRP below the cavitation threshold (0.5 MPa), to detach the nanobubble without causing inertial cavitation. Then, the PRP was increased above the cavitation threshold to verify the induction of inertial cavitation. Cavitation doses recorded during the US exposure are shown in Figure 5a. During the initial continuous US exposure with PRP below the cavitation threshold, no broad band noise was recorded, confirming the absence of inertial cavitation. Then, 100 cycles of US with a PRP above the cavitation threshold were applied (the moment in which the high-pressure 100-cycles pulse was applied is marked with an asterisk in Figure 5a). The cavitation dose recorded during the high-pressure 100-cycles pulse was drastically reduced compared to the cavitation dose obtained without the continuous US step. Moreover, increasing the duration of the continuous US step, the final cavitation dose was further reduced (Figure 5b). These results suggest that during the initial continuous US step nanobubbles adsorbed on the NC surface can be detached and then dissolved without causing inertial cavitation. Then, during the final 100-cycles pulse, only few NCs had nanobubbles on their surfaces, thus resulting in a low total cavitation dose.

3.5 Re-adsorption of gas nuclei makes amino-propyl functionalized ZnO NCs rechargeable

To understand if the process of gas adsorption on the nanocrystals surface could be reversed, the ultrasound sequence depicted in the inset of Figure 6a was used to expose the water solution containing the ZnO-NH_2 NCs. This is composed of 2 trains of pulses, each train composed of 5 pulses of 100-cycles each (PRF=1Hz). The idea behind the design of this ultrasound sequence is to first remove the nanobubbles on the ZnO NCs surface during the first ultrasound train (i.e. during the first 5 pulses of 100-cycles each) by causing them to detach and cavitate. Then, by setting an off-time (t_2) between the two ultrasound trains, to allow the re-adsorption of gas on the NC surface, and, eventually, by applying the second US train, to test the ability of the re-adsorbed gas to induce inertial cavitation. Actually, our hypothesis was that the gas dissolved in solution could re-adsorb over time at the NC surface, restoring its ability to induce inertial cavitation upon ultrasound exposure. Moreover, to test if the time between the ultrasound trains could influence the quantity of re-adsorbed gas, different off-times were tested. Using a PRP = 1.2 MPa, cavitation was detected only when ZnO-NH_2 were present in solution. Figure 6a shows the cavitation dose detected by PCD during the first 100-cycles pulse applied after the corresponding off-time t_2 (corresponding to the pulse marked with the asterisk in the inset of Figure 6a). With an off-time = 0 s, inertial cavitation was not detected, suggesting that all the adsorbed gas detached and cavitated during the first 5 pulses. By increasing the off-time from 30 up to 600 seconds, the ability of ZnO-NH_2 NCs to induce inertial cavitation was completely restored to the initial value of cavitation dose. This can be explained by the process of re-adsorption

of dissolved gases in solution at the ZnO-NH_2 nanocrystals surface, that, once re-exposed to ultrasound, induces again inertial cavitation. Indeed, the kinetics of the cavitation dose over Off-time resembles the kinetic rate described by the Elovich equation for gas adsorption onto a solid, where the adsorption rate of gases decreases exponentially with the amount of adsorbed gas [34, 35]. This result strongly suggests that it is possible to use ZnO-NH_2 nanocrystals to induce inertial cavitation repeatedly by allowing enough time to the dissolved gas in solution to re-adsorb at their surface. As it will be demonstrated below, it is pointed out that this behavior is strictly related to the presence of the NPs in solution.

To investigate the possibility to recharge the NCs surface with nanobubbles for multiple subsequent times, the ultrasound sequence depicted in Figure 6b was designed to expose the ZnO-NH_2 NCs. This is composed of 6 trains of pulses, each train composed by 5 pulses of 100 cycles each. As in the experiment discussed earlier, each train is used to completely detach and cavitate the nanobubbles at the surface of the NCs, while the off-time (t_2) is used to re-charge the nanobubble on the surface of the NCs. Different off-times have been used to evaluate the effect on the generated cavitation dose. Using a PRP = 1.2 MPa, cavitation was detected only when ZnO-NH_2 were present in the solution. Figure 6c shows the cavitation dose obtained during the first 100-cycles pulse of each of the 6 trains of pulses (corresponding to the pulses marked with an asterisk in Figure 6b) using off-times ranging from 30 seconds up to 600 seconds. Strikingly, an off-time equals to 600 seconds leads, for 5 consecutive times, to a cavitation dose equal to the one obtained during the first pulse of the first US train, suggesting a complete re-charge of the nanobubbles over the NCs surface during the off-times. On the contrary, shorter off-times lead to lower cavitation doses, suggesting that less gas was adsorbed on the NCs during the off-time. Interestingly, when using short off-times (from 30 s to 120 s), the same off-time repeated multiple consecutive times did not lead to the same cavitation dose. Indeed, the cavitation dose decreased over subsequent trains of pulses. This might be explained by considering the gas concentration in water over time. Indeed, ultrasound is known to degas liquids [58]: during several ultrasound trains, the total concentration of gas dissolved in the solution decreased, thus decreasing the gas adsorption on the NC surface that is dependent on the local concentration of gases. Together, these data strongly suggest the possibility to recharge the NCs surface with nanoubbles multiple subsequent times, thus allowing the re-generation of inertial cavitation up to 5 consecutive times.

3.6 Effect of different gases on the cavitation behavior

Next, the role that different types of gases have on the induction of inertial cavitation by ZnO-NH_2 NCs was explored. According to the same ultrasound exposure scheme previously shown (6 trains of pulses made by 5 100-cycles pulses each, off-time = 1 minute, Figure 6b), ZnO-NH_2 NCs were exposed to ultrasound in presence of different gases to study their influence on the NC recovery time, i.e. the time needed for the NCs to fully recover their cavitation-induction ability. Nitrogen (N_2), carbon dioxide (CO_2) and air were fluxed over the solution during the off-time before the ultrasound exposure in order to saturate the solution with the corresponding gas. The recorded cavitation dose during each 100-cycles-pulse is shown in Figure 7. Higher cavitation doses were obtained during the first pulse if nitrogen or air were fluxed over the solution before the ultrasound exposure: this can be explained by the fact that higher gas concentration, dissolved in the solution, resulted in an increase of the amount of gas adsorbed over the nanocrystal surface, thus leading to higher cavitation doses. Interestingly, fluxing CO_2 over the solution reduced the cavitation

dose obtained during the first pulse. Carbon dioxide is known to react with amine groups present over the surface of ZnO-NH_2 NCs. We hypothesize that the chemical reaction between molecular carbon dioxide and amine groups competes efficiently with the adsorption of carbon dioxide gas bubbles over the nanocrystal functionalized surface, finally reducing its ability to induce cavitation [59]. Notably, under air and nitrogen flux, even a short 30 seconds off-time was able to recover the 100% ability of ZnO-NH_2 NCs to induce inertial cavitation, against the 600 seconds without gas flux. This suggests that high gas concentrations in solution increased the adsorption rate of gas bubbles onto the ZnO-NH_2 NCs surface, further confirming the role of adsorbed gas on the induction of inertial cavitation. A similar value in the cavitation activity between N_2 and Air is also expected considering that recent studies have revealed that pure N_2 or O_2 have a only slight effect on the cavitation threshold in pulsed, focused, high energy ultrasonic field [36]. All-together these results confirm that the main mechanism behind the inertial cavitation induction by ZnO-NH_2 NCs is the adsorption of gases over their surface, and that nitrogen gas and air (actually composed by 78 %vol by nitrogen) results in higher cavitation doses.

3.7 ZnO-NH_2 NCs as novel echographic contrast agent

As a proof-of-concept, we exploited the use of ZnO-NH_2 NCs as echographic nano-contrast agents. B-mode images of pure water and ZnO-NH_2 NCs suspension in water were captured using a conventional diagnostic scanner for different PRP. Figure 8a shows the representative images of the nanocrystals suspension for PRP=1.6MPa, corresponding to a safe MI=1.6. Clearly, ZnO-NH_2 NCs generated a significant higher contrast intensity than water. Indeed, upon application of ultrasound, bright spots were immediately observed, confirming the bubbles production under ultrasound exposure. The bright spots disappeared immediately after ceasing ultrasound due to the short life-time of air bubbles in water. Supplementary videos are also provided to show the real-time response of the nanosystem to ultrasound irradiation, see the Supplementary Information. The presence of ZnO-NH_2 NCs resulted in higher ultrasound contrast intensities starting from 1.35MPa and MI=1.35 (Figure 8 b), thus showing the possibility to support ultrasound contrast imaging at safe mechanical indexes. Moreover, the increase of ZnO-NH_2 NCs concentration resulted in the increase of the number of cavitation bubbles (Figure 8c) and a subsequent higher contrast in B-mode images. Notably, even a nanocrystals concentration as low as 10 μg/mL was able to induce a detectable ultrasound contrast. Furthermore, ZnO-NH_2 NCs were able to induce continuous ultrasound contrast over 30 minutes (Figure 8d), although the intensity decayed gradually over time. Strikingly, this experiment shows much longer and sustained ultrasound contrast than that usually obtained using commercial microbubbles, typically enabling ultrasound contrast for less than 2 minutes [37]. Together, these measurements show the potential of ZnO-NH_2 NCs as novel ultrasound contrast nano-agents using safe and low mechanical index ultrasound excitation.

4. Conclusions

In the present study, we propose amino-propyl functionalized nanocrystals as novel nanoscale agents able to induce sustained and re-chargeable inertial cavitation by leveraging the adsorption of gas nanobubbles on their surface. When exposed to focused ultrasound of 1 MHz with PRP higher than 0.8 MPa, ZnO-NH_2 NCs promoted significantly higher inertial cavitation than water and pristine ZnO NCs solutions. Even concentrations as low as 12.5 μg/mL of ZnO-NH_2 NCs resulted in a detectable

inertial cavitation signal. By removing the adsorbed gas from the NCs surface by ethanol addition or degassing, we showed that the induction of inertial cavitation by ZnO-NH_2 NCs was due to nanobubbles adsorbed at their surface. Moreover, for the first time, we showed that gas nanobubbles, once displaced from the NC surface, could be re-adsorbed over time multiple times, re-activating the ability of ZnO-NH_2 NCs to induce inertial cavitation. Moreover, we showed that nanobubble adsorption is influenced by gas affinity with the surface, being nitrogen and air the ones most efficiently adsorbed on the surface. Finally, we showed that inertial cavitation induced by a safe level of ultrasound (MI < 1.9) generated up to 30 minutes of enhanced contrast in ultrasound imaging. Together, these results show the potential of ZnO-NH_2 NCs as novel nanoscale agents to repeatedly induce sustained cavitation over time, with applications ranging from diagnostic imaging to sonochemistry. Further future work, currently ongoing in our lab, will be needed to deepen the understanding of the mechanism behind their ability to generate inertial cavitation and to translate this technology into biomedical applications for in-vivo trials. In an effort toward a specifically targeted imaging nanoagent, the amino-propyl functionalization of the developed ZnO nanocrystals can be further equipped with peptides or antibodies enabling a preferential accumulation of the imaging contrast nanoagent into the diseased site of interest in-vivo.

Acknowledgements

This work has received funding from the European Research Council (ERC) under the European Union's Horizon 2020 research and innovation programme (grant agreement No 678151 – Project Acronym "TROJANANOHORSE" – ERC starting Grant).

Supplementary Information

Supplementary Information is available from Elsevier or from the authors. Nitrogen sorption measurements, real-time videos of the nano-system response to ultrasound irradiation are available, i.e. water-containing ZnO-NH_2 NCs (file name: *ZnO-NH2-1.6MPa*) and plain water as control (filename: *Water-1.6MPa*).

REFERENCES

[1] J. Condeelis, R. Weissleder, In Vivo Imaging in Cancer, Cold Spring Harb. Perspect. Biol., 2 (2010) a003848.

[2] J.Y. Lee, D. Carugo, C. Crake, J. Owen, M. de Saint Victor, A. Seth, C. Coussios, E. Stride, Nanoparticle-Loaded Protein–Polymer Nanodroplets for Improved Stability and Conversion Efficiency in Ultrasound Imaging and Drug Delivery, Adv. Mater., 27 (2015) 5484-5492.

[3] G. Canavese, A. Ancona, L. Racca, M. Canta, B. Dumontel, F. Barbaresco, T. Limongi, V. Cauda, Nanoparticle-assisted ultrasound: A special focus on sonodynamic therapy against cancer, Chem. Eng. J., 340 (2018) 155-172.

[4] S. Zullino, M. Argenziano, I. Stura, C. Guiot, R. Cavalli, From Micro- to Nano-Multifunctional Theranostic Platform: Effective Ultrasound Imaging Is Not Just a Matter of Scale, Mol. Imaging, 17 (2018) 1536012118778216.

[5] M. Wu, W. Chen, Y. Chen, H. Zhang, C. Liu, Z. Deng, Z. Sheng, J. Chen, X. Liu, F. Yan, H. Zheng, Focused Ultrasound-Augmented Delivery of Biodegradable Multifunctional Nanoplatforms for Imaging-Guided Brain Tumor Treatment, Adv. Sci., 5 (2018) 1700474.

Journal Pre-proofs

[6] R. Zhang, F. Yan, Y. Chen, Exogenous Physical Irradiation on Titania Semiconductors: Materials Chemistry and Tumor-Specific Nanomedicine, Adv. Sci., 5 (2018) 1801175-1801175.
[7] H. Tang, Y. Zheng, Y. Chen, Materials Chemistry of Nanoultrasonic Biomedicine, Adv. Mater., 29 (2017) 1604105.
[8] Z. Xing, J. Wang, H. Ke, B. Zhao, X. Yue, Z. Dai, J. Liu, The fabrication of novel nanobubble ultrasound contrast agent for potential tumor imaging, Nanotechnology, 21 (2010) 145607.
[9] D.G. Shchukin, E. Skorb, V. Belova, H. Möhwald, Ultrasonic Cavitation at Solid Surfaces, Adv. Mater., 23 (2011) 1922-1934.
[10] X.H. Zhang, N. Maeda, V.S.J. Craig, Physical Properties of Nanobubbles on Hydrophobic Surfaces in Water and Aqueous Solutions, Langmuir, 22 (2006) 5025-5035.
[11] M. Alheshibri, J. Qian, M. Jehannin, V.S.J. Craig, A History of Nanobubbles, Langmuir, 32 (2016) 11086-11100.
[12] A. Yildirim, R. Chattaraj, N.T. Blum, G.M. Goldscheitter, A.P. Goodwin, Stable Encapsulation of Air in Mesoporous Silica Nanoparticles: Fluorocarbon-Free Nanoscale Ultrasound Contrast Agents, Adv. Health. Mater., 5 (2016) 1290-1298.
[13] T. Uchida, S. Oshita, M. Ohmori, T. Tsuno, K. Soejima, S. Shinozaki, Y. Take, K. Mitsuda, Transmission electron microscopic observations of nanobubbles and their capture of impurities in wastewater, Nanoscale Res. Lett., 6 (2011) 295.
[14] N. Nirmalkar, A.W. Pacek, M. Barigou, On the Existence and Stability of Bulk Nanobubbles, Langmuir, 34 (2018) 10964-10973.
[15] J. Qiu, Z. Zou, S. Wang, X. Wang, L. Wang, Y. Dong, H. Zhao, L. Zhang, J. Hu, Formation and Stability of Bulk Nanobubbles Generated by Ethanol–Water Exchange, ChemPhysChem, 18 (2017) 1345-1350.
[16] Z. Fang, L. Wang, X. Wang, L. Zhou, S. Wang, Z. Zou, R. Tai, L. Zhang, J. Hu, Formation and Stability of Surface/Bulk Nanobubbles Produced by Decompression at Lower Gas Concentration, The Journal of Physical Chemistry C, 122 (2018) 22418-22423.
[17] Y. Zhou, X. Han, X. Jing, Y. Chen, Construction of Silica-Based Micro/Nanoplatforms for Ultrasound Theranostic Biomedicine, Adv. Health. Mater., 6 (2017) 1700646.
[18] J.J. Kwan, S. Graham, R. Myers, R. Carlisle, E. Stride, C.C. Coussios, Ultrasound-induced inertial cavitation from gas-stabilizing nanoparticles, Phys. Rev. E, 92 (2015) 023019.
[19] Q. Jin, S.-T. Kang, Y.-C. Chang, H. Zheng, C.-K. Yeh, Inertial cavitation initiated by polytetrafluoroethylene nanoparticles under pulsed ultrasound stimulation, Ultrason. Sonochem., 32 (2016) 1-7.
[20] J.J. Kwan, G. Lajoinie, N. de Jong, E. Stride, M. Versluis, C.C. Coussios, Ultrahigh-Speed Dynamics of Micrometer-Scale Inertial Cavitation from Nanoparticles, Phys. Rev. Appl., 6 (2016) 044004.
[21] A. Yildirim, R. Chattaraj, N.T. Blum, A.P. Goodwin, Understanding Acoustic Cavitation Initiation by Porous Nanoparticles: Toward Nanoscale Agents for Ultrasound Imaging and Therapy, Chem. Mater., 28 (2016) 5962-5972.
[22] X. Wang, H. Chen, Y. Chen, M. Ma, K. Zhang, F. Li, Y. Zheng, D. Zeng, Q. Wang, J. Shi, Perfluorohexane-Encapsulated Mesoporous Silica Nanocapsules as Enhancement Agents for Highly Efficient High Intensity Focused Ultrasound (HIFU), Adv. Mater., 24 (2012) 785-791.
[23] M. Zhang, J.R.T. Seddon, Nanobubble–Nanoparticle Interactions in Bulk Solutions, Langmuir, 32 (2016) 11280-11286.

Journal Pre-proofs

[24] A. Yildirim, D. Shi, S. Roy, N.T. Blum, R. Chattaraj, J.N. Cha, A.P. Goodwin, Nanoparticle-Mediated Acoustic Cavitation Enables High Intensity Focused Ultrasound Ablation Without Tissue Heating, ACS Appl. Mater. Interf., 10 (2018) 36786-36795.
[25] C. Pellow, D.E. Goertz, G. Zheng, Breaking free from vascular confinement: status and prospects for submicron ultrasound contrast agents, Wiley Interdiscip. Rev.: Nanomed. Nanobiotechnol., 10 (2018) e1502.
[26] M. Laurenti, G. Canavese, A. Sacco, M. Fontana, K. Bejtka, M. Castellino, C.F. Pirri, V. Cauda, Nanobranched ZnO Structure: p-Type Doping Induces Piezoelectric Voltage Generation and Ferroelectric–Photovoltaic Effect, Adv. Mater., 27 (2015) 4218-4223.
[27] M. Laurenti, S. Stassi, M. Lorenzoni, M. Fontana, G. Canavese, V. Cauda, C.F. Pirri, Evaluation of the piezoelectric properties and voltage generation of flexible zinc oxide thin films, Nanotechnology, 26 (2015) 215704.
[28] N. Garino, T. Limongi, B. Dumontel, M. Canta, L. Racca, M. Laurenti, M. Castellino, A. Casu, A. Falqui, V. Cauda, A Microwave-Assisted Synthesis of Zinc Oxide Nanocrystals Finely Tuned for Biological Applications, Nanomaterials, 9 (2019) 212.
[29] T. Þen, O. Tüfekçioðlu, Y. Koza, Mechanical index, Anatol J Cardiol, 15 (2015) 334-336.
[30] B. Dumontel, M. Canta, H. Engelke, A. Chiodoni, L. Racca, A. Ancona, T. Limongi, G. Canavese, V. Cauda, Enhanced biostability and cellular uptake of zinc oxide nanocrystals shielded with a phospholipid bilayer, J. Mater. Chem. B, 5 (2017) 8799-8813.
[31] G.L. J. J. Kwan, N. de Jong, E. Stride, M. Versluis, and C. C. Coussios, Ultrahigh-Speed Dynamics of Micrometer-Scale Inertial Cavitation from Nanoparticles, Physical review applied 6(2016).
[32] A.S. Konstantin Tamarov, Wujun Xu, Markus Malo, Valery Andreev, Victor Timoshenko, Vesa-Pekka Lehto, Nano Air Seeds Trapped in Mesoporous Janus Nanoparticles Facilitate Cavitation and Enhance Ultrasound Imaging, ACS Appl. Mater. Interfaces, 9 (2017).
[33] A.K. Kota, G. Kwon, A. Tuteja, The design and applications of superomniphobic surfaces, NPG Asia Mater. , 6 (2014) e109.
[34] Y. Ho, Review of second-order models for adsorption systems., J. Hazard. Mater. , 136 (2006) 681–689.
[35] I.S. Mclintock, The Elovich Equation in Chemisorption Kinetics, Nature 216 (1967) 1204–1205.
[36] B. Li, Y. Gu, M. Chen, An experimental study on the cavitation of water with dissolved gases, Exp Fluids, 12 (2017).
[37] Q. Jin, C.-Y. Lin, S.-T. Kang, Y.-C. Chang, H. Zheng, C.-M. Yang, C.-K. Yeh, Superhydrophobic silica nanoparticles as ultrasound contrast agents, Ultrason. Sonochem., 36 (2017) 262-269.

Journal Pre-proofs

Figures

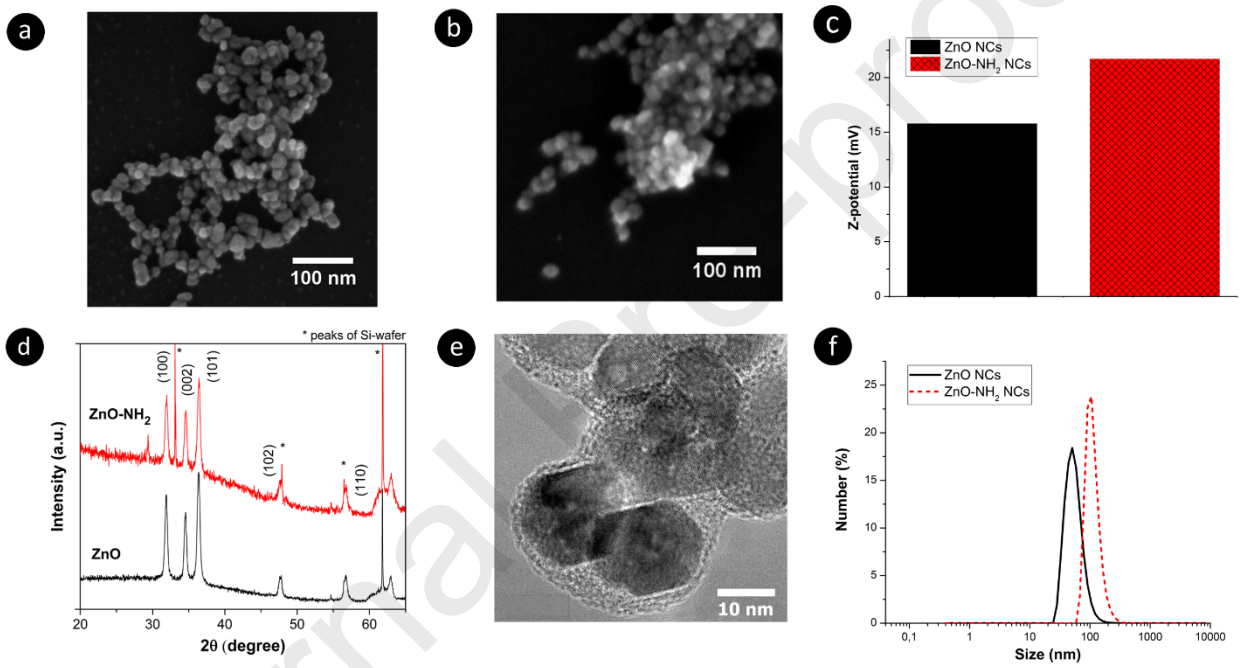

Figure 1. FESEM images of: (a) pristine ZnO NCs and (b) amino-propyl functionalized ZnO NCs. The NCs were all coated by a thin layer of Pt. (c) Z-Potential measurements of the NCs in water media; (d) Representative X-ray diffractograms of the ZnO NCs: pristine (black curve) and amino-propyl functionalized ones (red curve). (e) TEM image of ZnO-NH_2 NCs. (f) Dynamic Light Scattering size distributions of pristine (in black) and amino-propyl functionalized (in red) ZnO NCs

Journal Pre-proofs

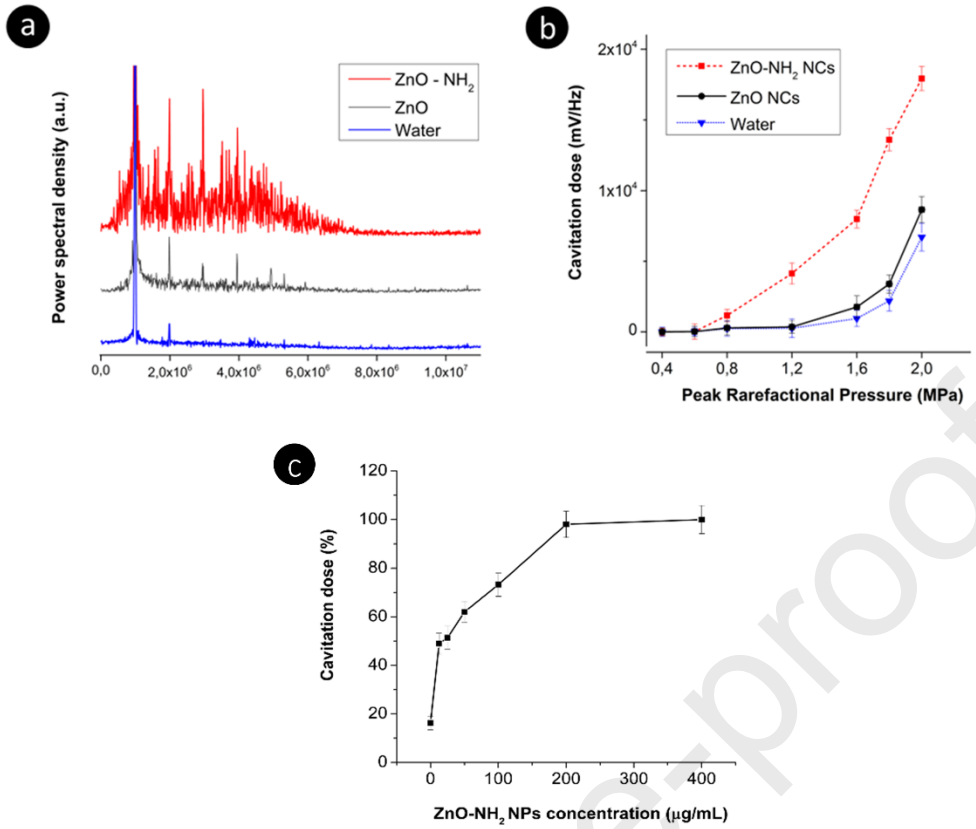

Figure 2. Passive cavitation detection measurements for bare (in black), amino-propyl functionalized (in red) ZnO NCs (200 µg/mL) containing solutions and water (in blue) under 985 KHz focused ultrasound excitation. (a) Plot of power spectral densities obtained for the three samples for a single 100-cycles-pulse at 1.8 MPa PRP. (b) Cavitation doses obtained varying the PRP from 0.4 MPa up to 2 MPa for the three samples. (c) Cavitation doses obtained varying the concentration of amino-propyl functionalized ZnO NCs normalized over the cavitation dose obtained at 400 µg/mL.

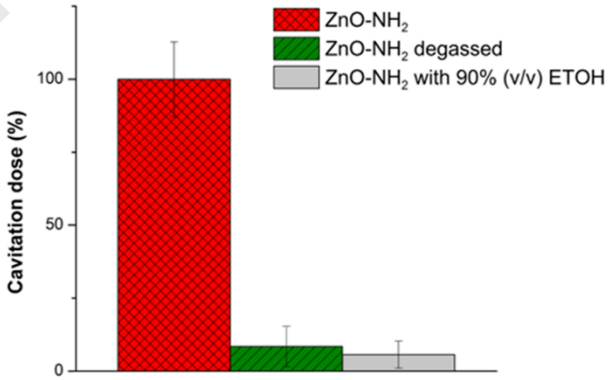

Figure 3. Effect of degassing and ethanol addition on the ability to induce inertial cavitation from amino-propyl functionalized ZnO NCs. Ultrasound conditions: single pulse of 100 cycles, PRP = 1.2 MPa, frequency = 1 MHz.

Journal Pre-proofs

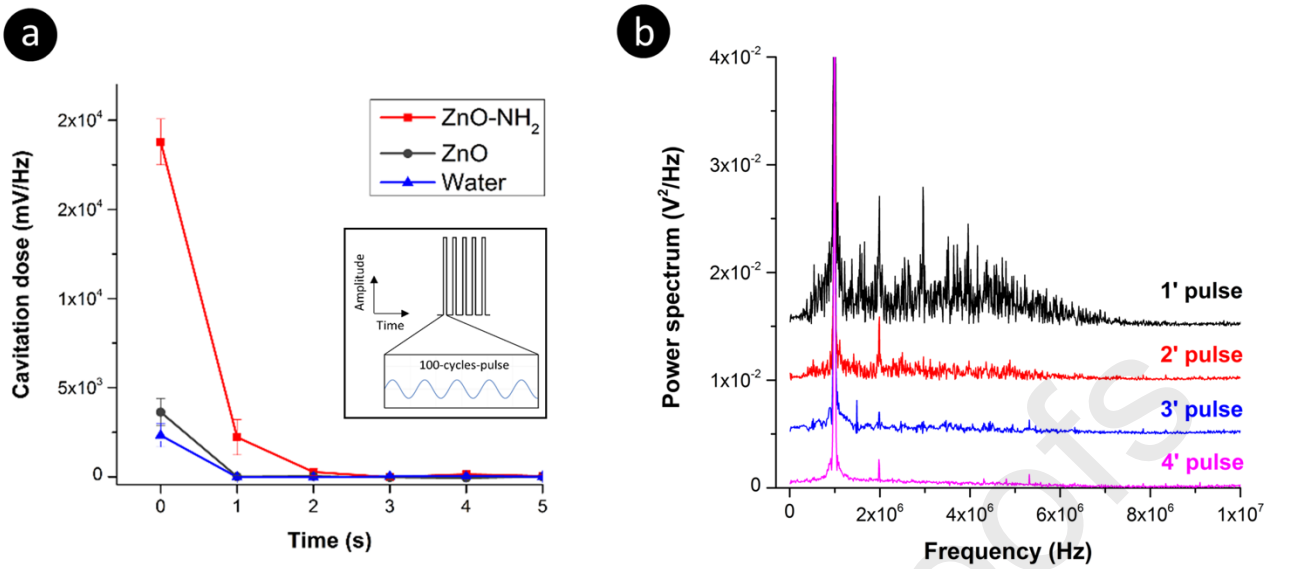

Figure 4. Passive cavitation measurements of pristine (black curves), amino-propyl functionalized (red curves) ZnO NCs solutions and water (blue curve) exposed to multiple 100-cycle-pulses. (**a**) Inset: Ultrasound train of 5 pulses with a PRF = 1 Hz, each pulse composed by 100 cycles. Quantified cavitation dose obtained for each 100-cycle-pulse over time (PRF = 1 Hz, PRP = 1.8 MPa). Time = 0s corresponds to the arrival of the first pulse to the sample. (**b**) Representative power spectral densities of the first four successive 100-cycles-pulses for the sample containing amino-propyl functionalized ZnO NCs.

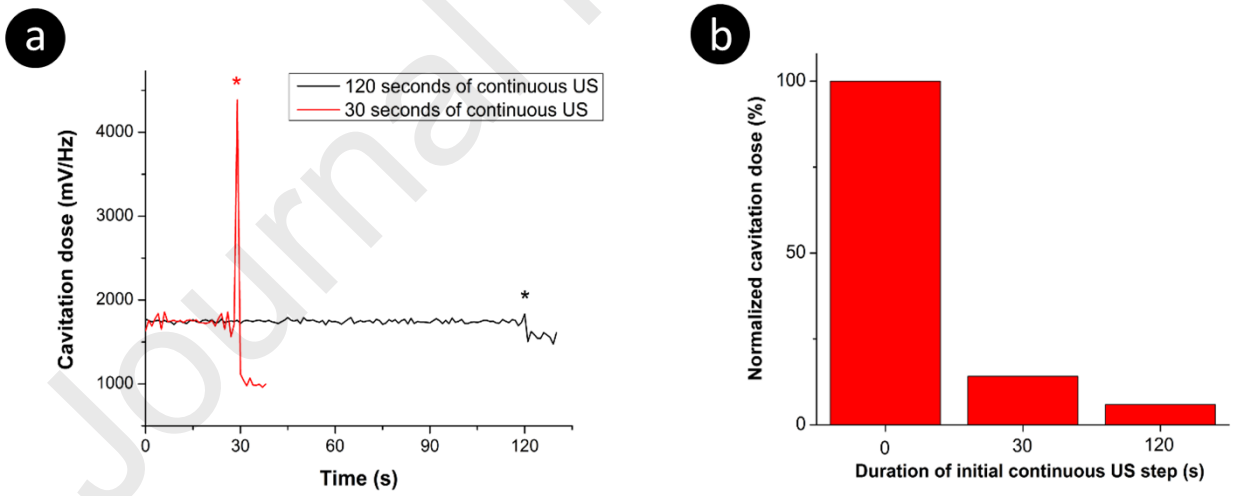

Figure 5. (a) Quantified cavitation dose over time obtained during initial continuous US exposure at PRP = 0.5 MPa and final 100-cycle-pulse (marked with an asterisk) at PRP = 1.6 MPa. (b) Quantified cavitation dose obtained during the 100-cycle-pulse at 1.6 MPa normalized to the cavitation dose obtained without the initial continuous US step. Different durations of continuous ultrasound with PRP below the cavitation threshold (PRP= 0.6 MPa) were used.

Journal Pre-proofs

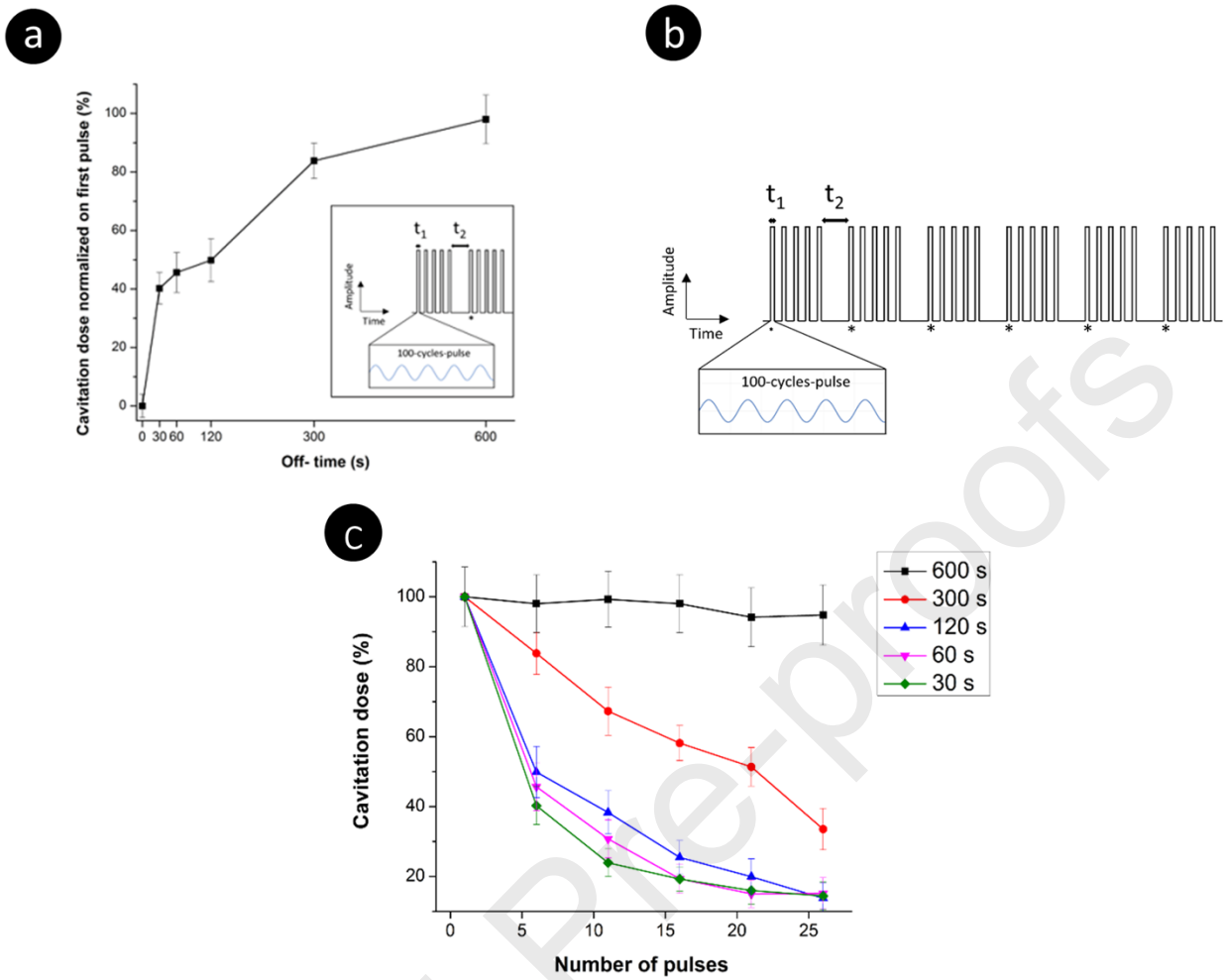

Figure 6. Passive cavitation measurements of amino-propyl functionalized ZnO NCs water solutions exposed to focused ultrasound. PRP = 1.2 MPa (**a**) Inset: scheme of the ultrasound pulse applied to the NCs. 2 train of 5 pulses each were used. A time of 1 second was set between each pulse, while an off-time t_2 was applied in between the two ultrasound trains. Plot: dose recorded during the first 100-cycles-pulse of the second train of 5 100 cycles pulses for different Off-times (corresponding to the pulse of Figure 7a marked with an asterisk). (**b**) Scheme of the ultrasound pulse used to expose the sample: trains of 5 100-cycle-pulses with different Off-times (t_2); t_1 = 100 µs, composed by 100-cycles-pulse at 1 Hz PRF**.** (**c**) Cavitation dose obtained during each 100-cycles-pulse. 6 trains of 5 100-cycles-pulses were applied. Every 5 100-cycles-pulses an Off-time was applied. Off-time varied from 30 seconds up to 600 seconds.

Journal Pre-proofs

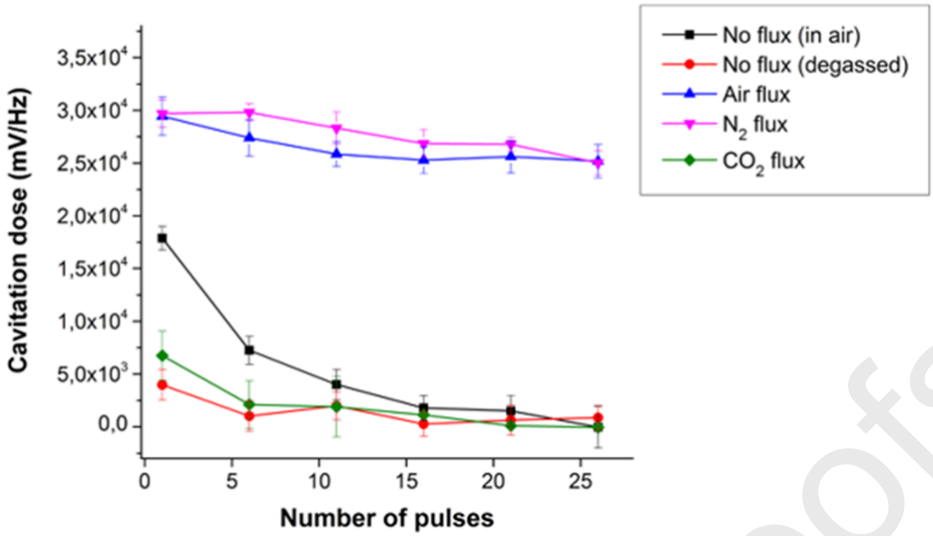

Figure 7. Passive cavitation measurements of amino-propyl functionalized ZnO nanocrystals exposed to 6 trains of 5 100-cycles-pulses each. Air, nitrogen and carbon dioxide gases were fluxed over the solution during the Off-time. Off-time = 1 minute, PRP = 1.2 MPa.

Journal Pre-proofs

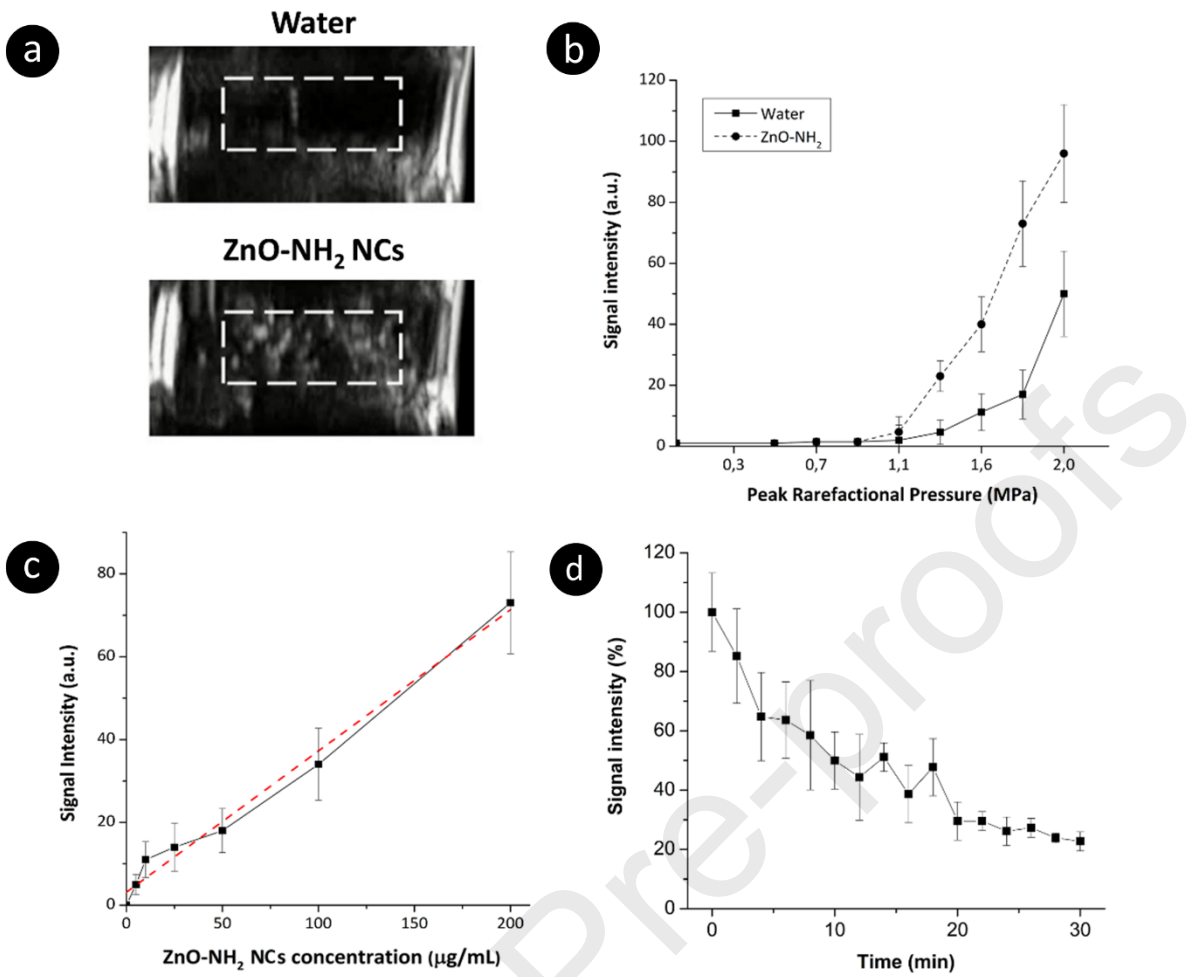

Figure 8. (a) Representative B-mode ultrasound images taken from movies acquired during ultrasound irradiation. White rectangles mark the region of interest (ROI) used for further quantification. White lateral stripes are due to reflection from the sample walls. (b) Quantified echographic signals for different PRPs for water and ZnO-NH_2 NCs (200 µg/mL) suspension. Error bars=1SD. (c) Quantified echographic signals for different ZnO-NH_2 NCs concentrations. (d) Normalized average intensities from the acquired movies over the irradiation time. Used ultrasound parameters in all experiments: PRF=10 Hz, DC= 10%, PRP=1.6MPa, experiments run in triplicate.

Journal Pre-proofs

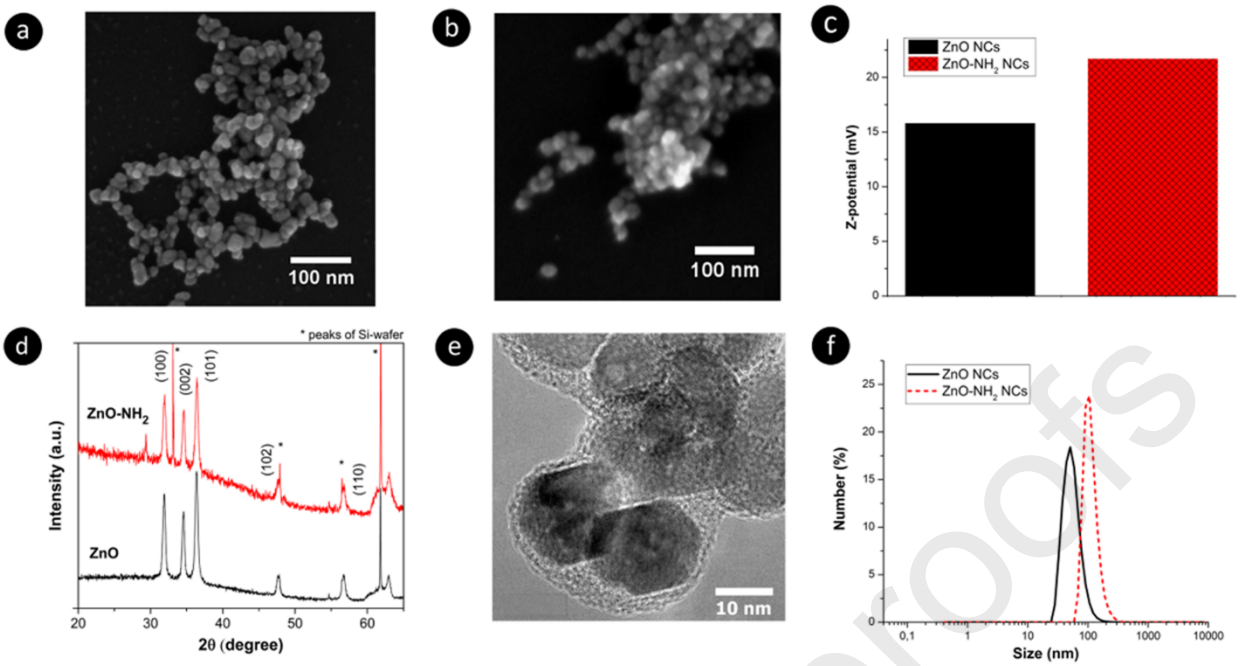

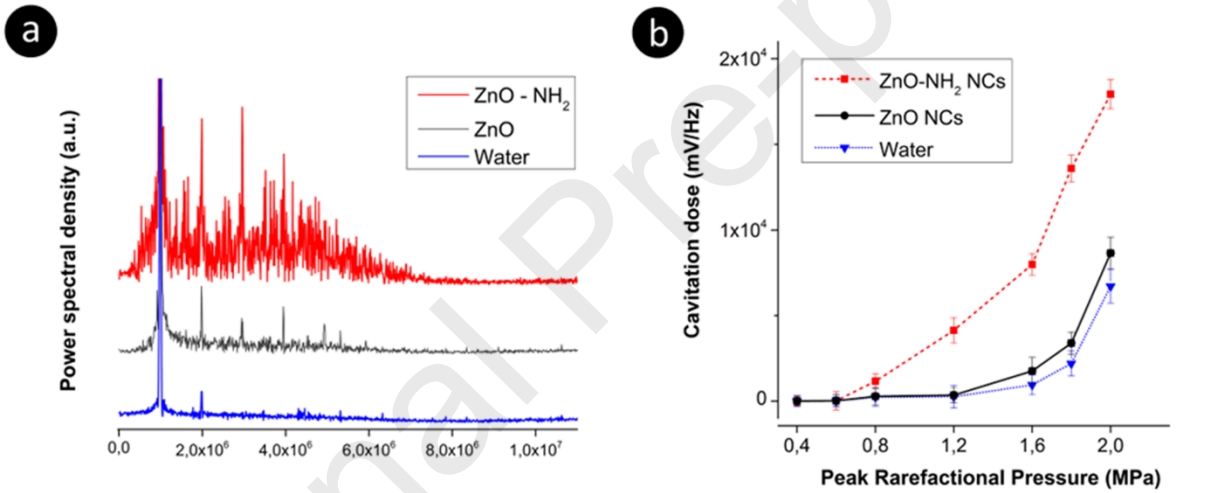

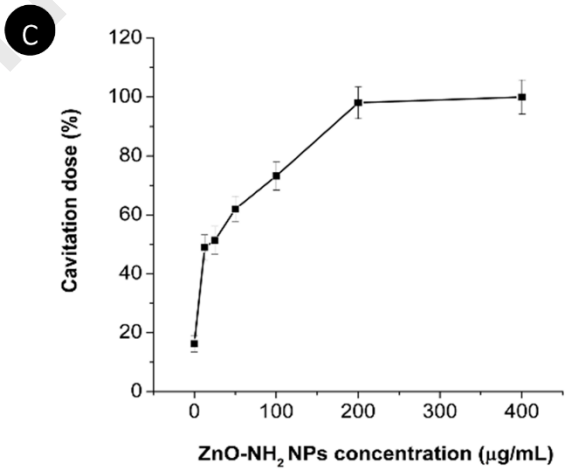

Journal Pre-proofs

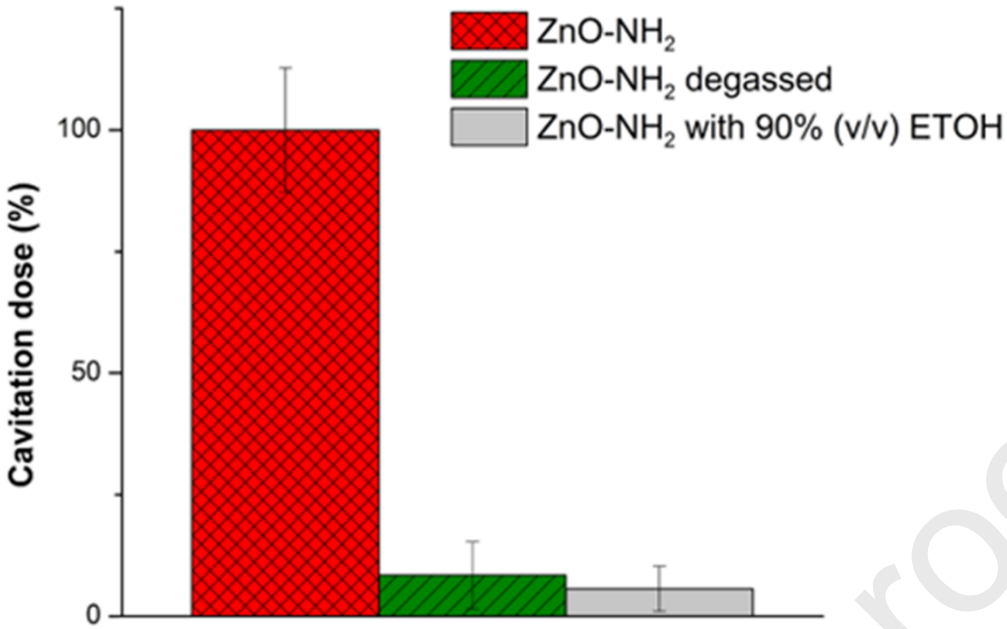

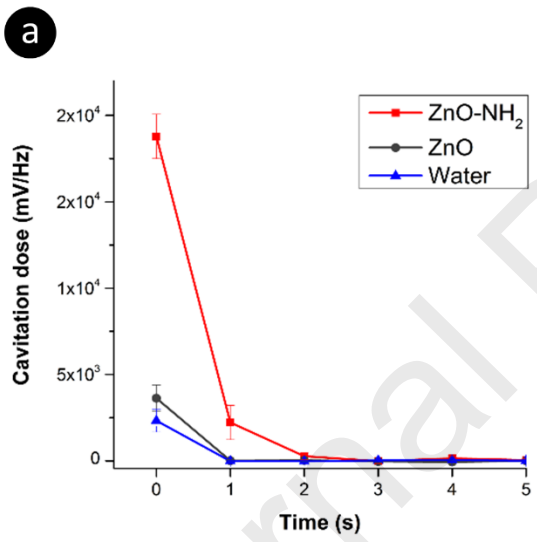

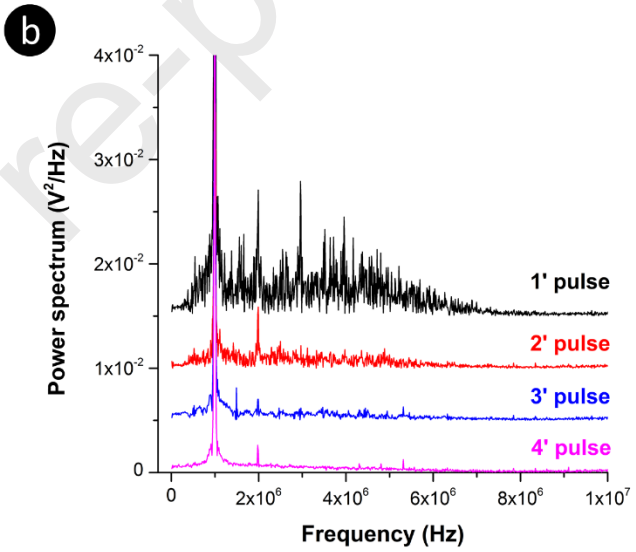

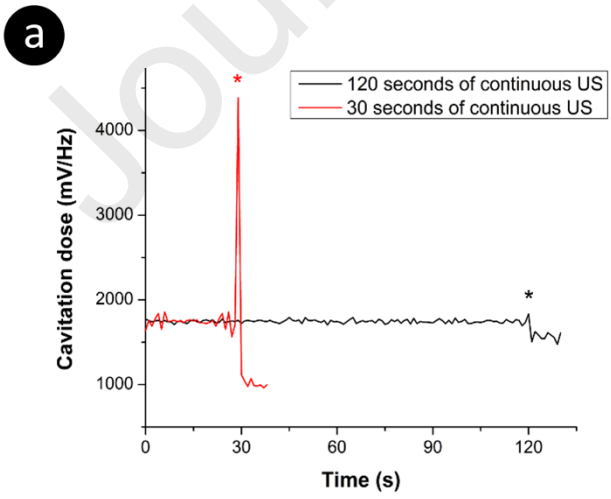

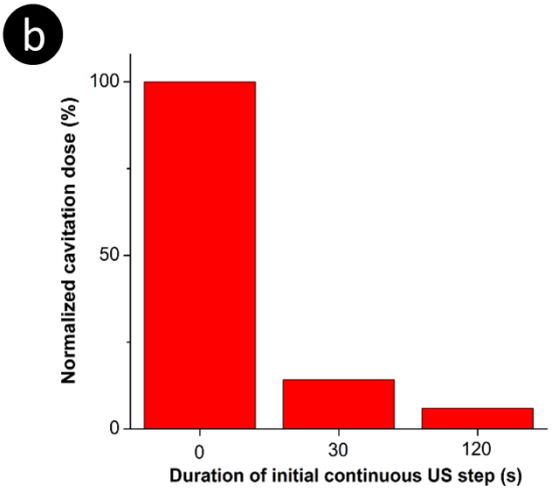

Journal Pre-proofs

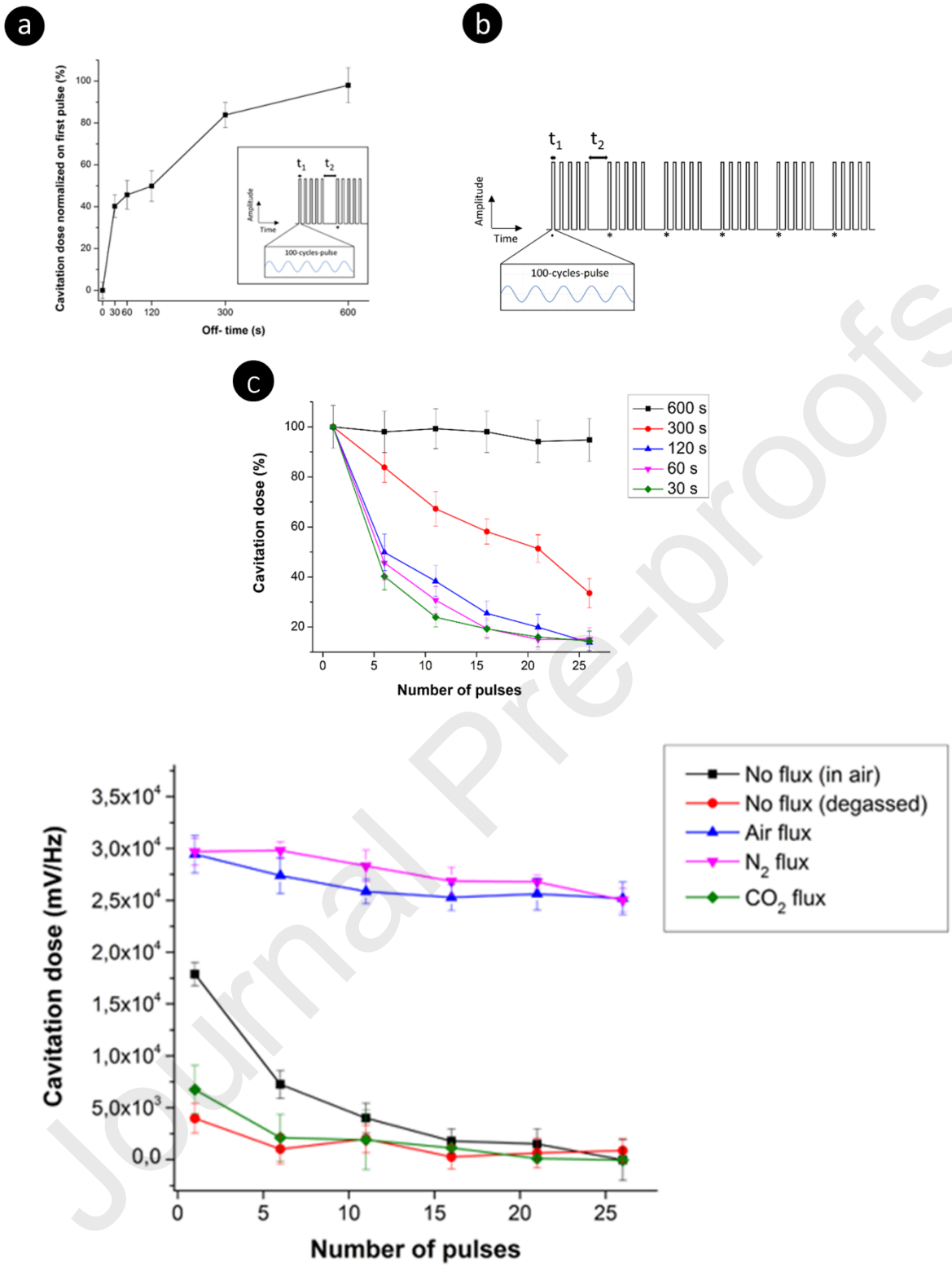

Journal Pre-proofs

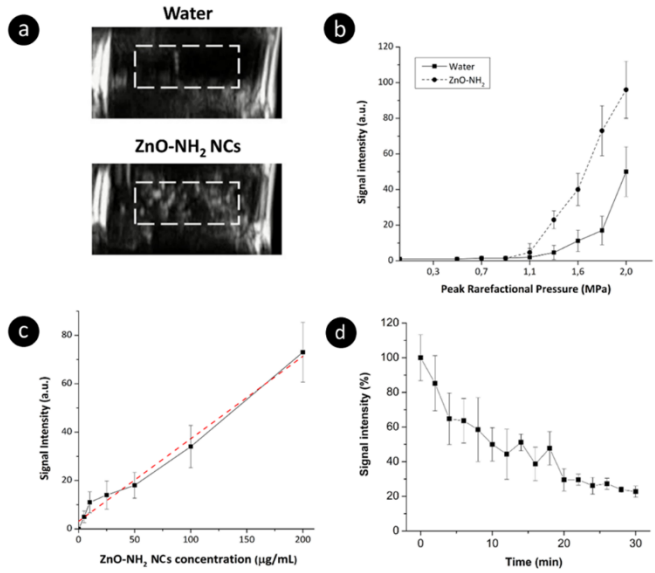

Leveraging re-chargeable nanobubbles on amine-functionalized ZnO nanocrystals for sustained ultrasound cavitation towards echographic imaging

Andrea Ancona, Adriano Troia, Nadia Garino, Bianca Dumontel, Valentina Cauda and Giancarlo Canavese*

Author Statement

NG and BD synthesized and functionalized the nanocrystals and performed the characterization experiments of figure 1, AA performed all the experiments related to acoustic cavitation and drafted the whole manuscript, AT supported the experiments with the use of cavitometer and imaging, GC and VC conceived the work and GC supervised all the experiments, VC was the grant recipient, all authors contributed to the manuscript editing.

Highlights

1) Novel nanoscale contrast agents able to induce a repeated and over-time sustained inertial cavitation

2) Zinc Oxide NanoCrystals (ZnO NCs) are opportunely functionalized with amino-propyl groups

3) ZnO NCs are also able to enhance echographic contrast signal (ECS)

4) Adsorption of gas on the NCs surface is responsible for this unprecedented rechargeable IC

5) Sustained IC and significant ECS obtained at physiologically relevant US conditions

Journal Pre-proofs

Journal Pre-proofs

Leveraging re-chargeable nanobubbles on amine-functionalized ZnO nanocrystals for sustained ultrasound cavitation towards echographic imaging

Andrea Ancona, Adriano Troia, Nadia Garino, Bianca Dumontel, Valentina Cauda and Giancarlo Canavese*

Author Statement
Authors declare no conflict of interest.

Journal Pre-proofs